Energy spectrum of rhombohedral III-V-VI_2 compounds: ternary isoelectronic analogues of bismuth-type semimetals

1990 J. Phys.: Condens. Matter 2 1129

(http://iopscience.iop.org/0953-8984/2/5/007)

J. Phys.: Condens. Matter **2** (1990) 1129–1140. Printed in the UK

Energy spectrum of rhombohedral III–V–VI_2 compounds: ternary isoelectronic analogues of bismuth-type semimetals

D V Gitsu, V G Kantser, N M Malkova and V A Tofan
Institute of Applied Physics, Academy of Sciences of the Moldavian SSR, Grosul 5, Kishinev 277028, USSR

Received 26 July 1988, in final form 4 July 1989

Abstract. A model of the electronic energy spectrum for the rhombohedral III–V–VI_2 compounds (the ternary isoelectronic analogues of the bismuth-type semimetals and the IV–VI semiconductors) has been elaborated on the basis of the genesis of their crystalline structure from the simple cubic lattice as well as the derivation of the band spectrum from the atomic p states. Rhombohedral III–V–VI_2 compounds are shown to be narrow-gap semiconductors, with two conduction and two valence bands located at Γ- and L points of the Brillouin zone. The band structure of $TlBiC_2^{VI}$ compounds has been found to be normal, while that of $TlSbC_2^{VI}$ is inverted.

1. Introduction

The calculation of the electron energy spectra of crystals is perhaps the oldest problem of solid-state quantum physics. Over a period of more than 30 years numerous methods have been elaborated for describing the electronic structure of solids. The tight-binding method of Stater and Koster [1] has achieved great popularity at present. The interactions of the Slater–Koster Hamiltonian may be calculated directly, but more frequently they are treated as empirical parameters found from experimental data. Many investigations have been made for the average valence four, or ⟨IV⟩, semiconductors [2].

Nevertheless, the construction of the similar models has been initiated for the average valence five, or ⟨V⟩, crystals, i.e. the group V elements (bismuth-type semimetals) and the IV–VI narrow-band-gap semiconductors [3]. The crystal structure of these ⟨V⟩ materials is similar to the simple cubic (SC) lattice and differs from it by smaller structural distortion or by slight non-equivalence of atoms in the components. In addition in these materials the bands near the Fermi energy are generated primarily from the atomic states of p symmetry [4]. On this basis Pankratatov and Volkov [3] found that electron spectra of the bismuth-type semimetals and the IV–VI narrow-gap semiconductors can be reasonably well obtained from the universal spectrum of the parent phase, i.e. a hypothetical metal with a SC lattice and three overlapping p bands. Taking into account the p character of the bands they refer to this band-structure model as the p model [3].

In this paper we present a generalisation of the p model [3] for describing the electronic structure of the III–V–VI_2 compounds, which also belong to the average valence five crystals and are ternary isoelectronic analogues of the bismuth-type semimetals and the IV–VI semiconductors.

0953-8984/90/051129 + 12 $03.50

The experimental investigation of the III–V–VI_2 compounds started a comparatively long time ago [5]. At present data are available for nine III–V–VI_2 compounds with III ≡ Tl; V ≡ Bi, Sb, As; VI ≡ S, Se, Te. As a rule $TlAsC_2^{VI}$ compounds are glass-like [6]. The compounds with Bi and Sb are crystalline [7], with $TlBiC_2^{VI}$ and $TlSbTe_2$ having rhombohedral symmetry D_{3d} under usual conditions [8], while $TlSbS_2$ and $TlSbSe_2$ crystallise in a lattice of lower symmetry [9].

Thus, among the III–V–VI_2 compounds the rhombohedral crystalline structure is the simplest, as in the IV–VI rocksalt structure. That is why they have previously been experimentally investigated more intensively [10] (especially $TlBiTe_2$, which is regarded as a good thermo- and acoustoelectric material [11]).

According to the limited experimental data available, the rhombohedral $TlB^VC_2^{VI}$ compounds are degenerate narrow-gap semiconductors with anisotropic physical properties [12]. For example, the energy gap for $TlBiTe_2$ obtained in [13] is 0.11 eV. However, this value as well as the value of the effective mass density-of-states is derived in the frame of the IV–VI semiconductor band model, though experimental data concerning the transport properties indicate that the compound has a more complex energy spectrum.

This situation imposes new demands on the model being developed here, i.e. the need to predict the band structure of the III–V–VI_2 compounds, to explain the nature of small gaps, to discover the points of the band extrema localisation in $\boldsymbol{k}$ space, as well as to identify the scaling in the isoelectronic series of the ⟨V⟩ crystals. The usual way to fit the bands of an isoelectronic series of compounds is first to fit the bands of the elementary crystals where scaling is seen more easily, and then to use these parameters to fit the bands of the more complex compounds which have a greater number of disposable parameters. The p model [3] for describing the electronic structure of cubic-like crystals permits the realisation of such an analysis. Our model based on the ideas of the p model [3] has the following properties:

(i) the chemistry of p-bonding in the cubic-like ⟨V⟩ crystals [4] is preserved

(ii) the main part of the matrix elements is related to the atomic energies and the parameters of the chemical constituents, permitting exploration of chemical trends and simple treatment of alloys

(iii) the model employs a minimum number of parameters to describe the band structure of the III–V–VI_2 compounds and their alloys.

In § 2 we present an analysis of the structure of III–V–VI_2 compounds; the model Hamiltonian and its matrix elements are discussed in § 3. The resulting energy spectrum in vicinity of the Γ- and the L-points of the Brillouin zone is presented in § 4. The model parameters and energy gaps of the III–V–VI_2 compounds are discussed in § 5.

2. Crystal lattice and Brillouin zone

The structure analysis of the presently known III–V–VI_2 compounds has shown that they have an octahedral atomic arrangement which is characteristic of the IV–VI compounds and the bismuth-type semimetals. This is due to the cubic symmetry of the valent bonds of the V-group elements formed at p orbitals. The symmetry group of the III–V–VI_2 rhombohedral compounds is D_{3d}^5, the same as that of the bismuth-type semimetals. However, as their Bravais lattices are different the rhombohedral lattice of III–V–VI_2 compounds can be obtained from the SC one by slightly different operations than for Bi [14].

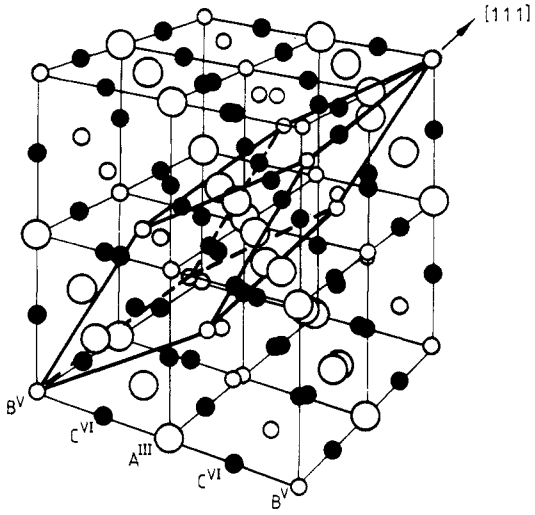

Figure 1. The unit cell of the III–V–VI$_2$ rhombohedral compounds $A^{III}B^VC_2^{VI}$ with A ≡ Tl, B ≡ Bi, Sb, As, C ≡ S, Se, Te.

Separating in the initial SC lattice two face-centred cubic (FCC) sublattices, at the first stage (as for IV–VI) we locate cations into the sites of one FCC sublattice and anions into the other. After that operation for the III–V–VI$_2$ compounds we obtain the disordered cubic phase with the rocksalt structure; it can be called the 'false rocksalt' lattice. For the rhombohedral phase of III–V–VI$_2$ two types of the cation atoms A^{III} and B^V are ordered in layers perpendicular to one of the cube body diagonals [111]. The latter leads to a doubling of the lattice period along [111] in comparison with IV–VI and to a reduction in symmetry from O_h^5 to D_{3d}^5.

The real III–V–VI$_2$ rhombohedral lattice is characterised by two additional elements: a displacement u of the anion atomic layers towards the layer of B^V atoms, which doubles the period of the anion sublattice, and a small rhombohedral shear ε along [111]. The displacement of atomic layers and rhombohedral shear are characteristic for Bi-type semimetals, these are just the factors that cause specificity of its physical properties.

If the shear strain and displacement of the anion layers are neglected, the III–V–VI$_2$ lattice of sites has the SC structure, its rhombohedral symmetry D_{3d} being connected with the complicated unit cell basis. We called such a lattice 'pseudo-cubic'. Its unit cell basis vectors (depicted by thick lines in figure 1) are $\boldsymbol{a}_1 = a(2, 1, 1)$, $\boldsymbol{a}_2 = a(1, 2, 1)$, $\boldsymbol{a}_3 = a(1, 1, 2)$ (where a is the SC lattice spacing). The number of the atoms in the unit cell is 4 (one A^{III} atom, one B^V and two C^{VI}), its volume is $4a^3$, that is four times larger than the SC lattice unit cell.

When analysing the structure, the rhombohedral lattice is characterised [15] by the length a_0 of the basis vectors and by the angle α between either two of them. The degree of distortion of the III–V–VI$_2$ real rhombohedral lattices from the pseudo-cubic one can be described by the relative displacement of the anion layers $u = 0.5 - 2x_c$ (x_c is chalcogen atom coordinate in the rhombohedral lattice) and by the relative change of the distance between the layers due to the rhombohedral shear strain $\varepsilon_{xy} = 0.5(\cos\alpha - \cos\alpha_c)/[1 + \cos\alpha_c(1 - 2\cos\alpha)]$ (α_c is the pseudo-cubic lattice rhombohedral angle). The numerical values of these parameters for $TlBiC_2^{VI}$ and $TlSbTe_2$ compounds are listed in table 1.

The basis vectors of the reciprocal lattice to the pseudo-cubic one are $b_1 = (\pi/2a)(3\bar{1}\bar{1})$, $b_2 = (\pi/2a)(\bar{1}3\bar{1})$, $b_3 = (\pi/2a)(\bar{1}\bar{1}3)$. The Brillouin zone constructed on

Table 1. The parameters of the crystal lattices and Brillouin zones for the III–V–VI_2 compounds.

Parameter	Pseudo-cubic lattice	$TlBiS_2$	$TlBiSe_2$	$TlBiTe_2$	$TlSbTe_2$
a (Å)	—	3.090	3.164	3.245	3.205
a_0 (Å)	—	7.651	7.832	7.137	8.177
α	33° 33.4′	31° 28′	31° 15′	32° 18′	31° 24′
x_c	0.250	—	—	0.246	0.243
ε_{xy}	0	0.0238	0.0264	0.0140	0.0246
u	0	—	—	0.008	0.014

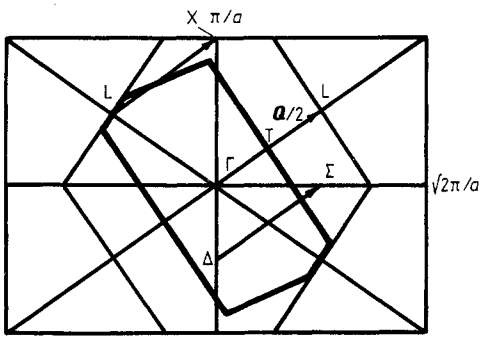

Figure 2. The sections of the SC, FCC and pseudo-cubic lattice Brillouin zones by the plane $k_x = k_y$.

them has the typical form for the rhombohedral lattices [15]. When passing to the deformed coordinate system the Brillouin zone coincides with that of the real III–V–VI_2 compounds. Its six L points with the coordinates $\pm(\pi/2a)(\bar{1}11)$, $\pm(\pi/2a)(1\bar{1}1)$, $\pm(\pi/2a)(11\bar{1})$ are located in the centres of six pseudo-square faces. Two points $((\pm\pi/4a)(111))$ are disposed in the centres of the hexagon faces. The centres of the remaining six pseudo-hexagon faces are placed in the middle of the $\boldsymbol{b}_i$ vectors. It is important to note that because of the doubling of the lattice period along [111] the L points are located two times further from the origin of the coordinates than the T points.

The sections of the Brillouin zones for the SC, FCC and pseudo-cubic lattices by the plane $k_x = k_y$ are shown in figure 2. In the figure the most symmetrical points are also shown, as well as their matching by the new reciprocal lattice vector $\boldsymbol{Q}/2 = (\pi/2a)(1, 1, 1)$ after the doubling of the lattice period.

3. The Hamiltonian, its matrix elements and secular determinant

When constructing the electronic energy bands in the frame of the p model [3] the parent phase with the initial SC lattice is considered first. Its energy spectrum is that of a metal. This fact can be explained if the parent phase spectrum is constructed in terms of the tight-binding method on the located p orbitals. On account of the triple degeneracy of the p level the energy spectrum consists of three overlapping bands which are degenerate at $\boldsymbol{k} = 0$ (if we neglect spin–orbit interaction). As the number of the valence p electrons per atom is three, all bands without mutual interaction are half-filled. Consequently, to endow dielectric properties to the spectrum it is necessary to double the lattice period

of the SC parent phase. The almost complete nesting of the parent phase Fermi surface is a precondition for that, the appearance of the gap being connected with the imposition on the SC lattice of some perturbation, which is considered to be known in the frame of the p model.

This perturbation is initiated by the SC lattice distortion in the Bi-type semimetals as well as in IV–VI semiconductors by the so-called ionic potential $\Delta(\boldsymbol{r})$ characterising the chemical difference of the metal and chalcogen atoms. The $\Delta(\boldsymbol{r})$ potential satisfies the following relations:

$$\begin{aligned} \Delta(\boldsymbol{r}+\boldsymbol{\rho}) &= \Delta(\boldsymbol{r}), \\ \Delta(\boldsymbol{r}+\boldsymbol{\tau}) &= -\Delta(\boldsymbol{r}), \end{aligned} \tag{1}$$

where $\boldsymbol{\rho}$ is the lattice vector of one of the FCC sublattice, and $\boldsymbol{\tau} = a(111)$.

In accordance with the general structure analysis the perturbation imposed on the parent phase of the III–V–VI$_2$ compounds includes several parts. The first is the first ionic potential $\Delta(\boldsymbol{r})$, which is completely equivalent to the IV–VI perturbation. It characterises the chemical difference between the chalcogen atom and the metal pseudo-atom $D^{IV} = \langle A^{III}B^{V}\rangle$ (that is, its physical characteristics are average between A^{III} and B^{V} ones). In order to take into account the cation ordering we introduce the second ionic potential $\Sigma(\boldsymbol{r})$ as the second part of the perturbation manifesting the chemical difference of two cation types. The $\Sigma(\boldsymbol{r})$ potential has translation periodicity of the rhombohedral lattice and it satisfies the following relations

$$\Sigma(\boldsymbol{r}+\boldsymbol{\pi}) = \Sigma(\boldsymbol{r}) \tag{2}$$

$$\Sigma(\boldsymbol{r}+2\boldsymbol{\tau}) = -\Sigma(\boldsymbol{r}) \tag{3}$$

where $\boldsymbol{\pi}$ is the rhombohedral lattice vector. With the origin of coordinates chosen at the cation atom the $\Delta(\boldsymbol{r})$ and $\Sigma(\boldsymbol{r})$ are even functions

$$\Delta(-\boldsymbol{r}) = \Delta(\boldsymbol{r}) \tag{4}$$

$$\Sigma(-\boldsymbol{r}) = \Sigma(\boldsymbol{r}). \tag{5}$$

The perturbations characterising the anion layer displacement $U(\boldsymbol{r})$ and rhombohedral deformation $\varepsilon(\boldsymbol{r})$ have the same form as for the semimetals [14]. However, in contrast to semimetals the $U(\boldsymbol{r})$ potential as well as $\Sigma(\boldsymbol{r})$ are even functions due to centring of the coordinate system at the cation rather than at the displacing layer [14]. The analysis shows that the remaining $U(\boldsymbol{r})$ symmetry properties coincide with the $\Sigma(\boldsymbol{r})$ ones, that allows us to unite them in the frame of the interpolation method. The united potential shall be designated by $\Sigma(\boldsymbol{r})$ symbol.

After inserting the deformation we have to pass to the deformed coordinate system [16] with the result that the Bravais lattices of the deformed and non-deformed crystals coincide. Therefore the translation periods of all enumerated potentials are unchanged and $\varepsilon(\boldsymbol{r})$ potential has the period of the SC lattice.

It is also convenient to divide the spin–orbit interaction into three parts $\Lambda(\boldsymbol{r})$, $\Lambda^{\Delta}(\boldsymbol{r})$, $\Lambda^{\Sigma}(\boldsymbol{r})$ caused by the $V(\boldsymbol{r})$ (the SC lattice potential), $\Delta(\boldsymbol{r})$ and $\Sigma(\boldsymbol{r})$, correspondingly.

Thus, the complete Hamiltonian for the model has the form

$$\hat{H} = \hat{H}_0 + \hat{\Lambda} + \hat{\varepsilon} + \hat{\Delta} + \hat{\Lambda}^{\Delta} + \hat{\Sigma} + \Lambda^{\Sigma} \tag{6}$$

where $\hat{H}_0 + \hat{\Lambda}$ is the SC lattice Hamiltonian.

In accordance with the p model the solution of the Schrödinger equation $\hat{H}\psi = E\psi$ is searched in the expansion form

$$\psi(\boldsymbol{r}) = \sum_{nk\sigma} u_{nk\sigma}\varphi_{nk\sigma}(\boldsymbol{r})$$

over the SC lattice Bloch functions constructed from the p orbitals

$$\varphi_{nk\sigma}(\boldsymbol{r}) = \frac{1}{\sqrt{N}} \sum_i \mathrm{e}^{\mathrm{i}\boldsymbol{k}\boldsymbol{R}_i} \rho_{n\sigma}(\boldsymbol{r} - \boldsymbol{R}_i). \tag{7}$$

Here the summation is carried out over N sites of the SC lattice, $p_{n\sigma}(\boldsymbol{r})$ are localised functions with p orbital symmetry, σ is a spin index, and the index $n = x, y, z$ numbers the p orbitals. The set of equations for determination of the energy spectrum and the wavefunction has the form

$$\sum_{nk\sigma} u_{nk\sigma} \langle \varphi_{n'k'\sigma'} | \hat{H} - E | \varphi_{nk\sigma} \rangle = 0. \tag{8}$$

Using only two nearest-neighbour interactions one obtains the Hamiltonian matrix of the deformed FCC lattice ($\hat{\Sigma} = \hat{\Lambda}^{\Sigma} = 0$)

$$\hat{H}(\boldsymbol{k}|\varepsilon) = \begin{bmatrix} \hat{\xi}(\boldsymbol{k}) + \hat{\eta}(\boldsymbol{k}) + \hat{W}(\boldsymbol{k}) + \hat{\Lambda} + \hat{\varepsilon}_0 + \hat{\varepsilon}(\boldsymbol{k}) & \hat{\Delta}_0 + \hat{\eta}^{\Delta}(\boldsymbol{k}) + \hat{W}^{\Delta}(\boldsymbol{k}) + \hat{\Delta}^{\Delta} \\ \hat{\Delta}_0 + \hat{\eta}^{\Delta}(\boldsymbol{k}) + \hat{W}^{\Delta}(\boldsymbol{k}) + \hat{\Lambda}^{\Delta} & -\hat{\xi}(\boldsymbol{k}) + \hat{\eta}(\boldsymbol{k}) + \hat{W}(\boldsymbol{k}) + \hat{\Lambda} + \hat{\varepsilon}_0 - \hat{\varepsilon}(\boldsymbol{k}) \end{bmatrix}. \tag{9}$$

All the above are 6×6 matrices with elements

$$\begin{aligned} \xi_{xx}(\boldsymbol{k}) &= \xi_0 \cos(k_x a) + \xi_1[\cos(k_y a) + \cos(k_z a)] \\ \eta^{(\Delta)}_{xx}(\boldsymbol{k}) &= \eta^{(\Delta)}_1 \cos(k_x a)[\cos(k_y a) + \cos(k_z a)] + \cos(k_y a)\cos(k_z a) \\ W^{(\Delta)}_{xy}(\boldsymbol{k}) &= W^{(\Delta)} \sin(k_x a)\sin(k_y a) \\ \varepsilon_{xy}(\boldsymbol{k}) &= \varepsilon_1[\cos(k_x a) + \cos(k_y a)] + \varepsilon_2 \cos(k_z a). \end{aligned} \tag{10}$$

The residual matrix elements are obtained from (10) by permutation of the cyclic indices. The matrix Δ_0 is diagonal ($\Delta_{0ij} = \Delta_0 \delta_{ij}$), $\hat{\varepsilon}_0$ is non-diagonal ($\varepsilon_{0ij} = \varepsilon_0(1 - \delta_{ij})$). The constants $\Delta_0, \xi_i, \eta_i, W, \eta_i^{\Delta}, W^{\Delta}, \varepsilon_i$ are the overlap integrals. These are model parameters [3]. All spin-orbital matrices have the same form [3]

$$\Lambda^{(\Delta,\Sigma)} = -\mathrm{i}\lambda^{(\Delta,\Sigma)} \begin{pmatrix} 0 & \hat{\boldsymbol{\sigma}}_z & -\hat{\boldsymbol{\sigma}}_y \\ -\hat{\boldsymbol{\sigma}}_z & 0 & \hat{\boldsymbol{\sigma}}_x \\ \hat{\boldsymbol{\sigma}}_y & -\hat{\boldsymbol{\sigma}}_x & 0 \end{pmatrix} \tag{11}$$

where $\hat{\boldsymbol{\sigma}}_n$ are the Pauli spin matrices, spinors are determined relative to the cubic axis z. The constants $\Lambda, \Lambda^{\Delta}, \Lambda^{\Sigma}$ are also model parameters.

Taking into account the properties (2)–(5) for the $\Sigma(\boldsymbol{r})$ matrix elements one obtains

$$\begin{aligned} \langle \varphi_{n'k'\sigma'} | \Sigma(\boldsymbol{r}) | \varphi_{nk\sigma} \rangle = \sum_j \mathrm{e}^{\mathrm{i}\boldsymbol{k}\boldsymbol{R}_j} [&\langle p_{n'}(\boldsymbol{r}) | \Sigma'(\boldsymbol{r}) | p_n(\boldsymbol{r} - \boldsymbol{R}_j) \rangle \delta_{k', k - Q/2} \\ &+ \langle p_{n'}(\boldsymbol{r}) | \Sigma'(-\boldsymbol{r}) | p_n(\boldsymbol{r} - \boldsymbol{R}_j) \rangle \delta_{k', k + Q/2}] \delta_{\sigma\sigma'} \end{aligned} \tag{12}$$

where

$$\Sigma'(\pm\boldsymbol{r}) = \tfrac{1}{2}[\Sigma(\boldsymbol{r}) \mp \mathrm{i}\Sigma(\boldsymbol{r} + \tau)]. \tag{13}$$

As follows from (12) the potential $\Sigma(\boldsymbol{r})$ results in interaction of the $\varphi_{n'k'\sigma'}$ and $\varphi_{nk\sigma}$ states separated by the $\boldsymbol{Q}/2$ vector in the $\boldsymbol{k}$ space. Consequently, one more quasi-diagonal block of the form (9) (replacing $\boldsymbol{k}$ with $\boldsymbol{k}-\boldsymbol{Q}/2$), and non-diagonal blocks $\Sigma(\boldsymbol{r})$ defined by the $\hat{\Sigma}$ and $\hat{\Lambda}^{\Sigma}$ potentials appear in the complete Hamiltonian.

Thus, the set of equation (8) in matrix form is

$$\begin{bmatrix} \hat{H}(\boldsymbol{k}|\varepsilon)-E\hat{\mathbf{I}}_{12} & \hat{\Sigma}(\boldsymbol{k}) \\ \hat{\Sigma}^{+}(\boldsymbol{k}) & \hat{H}(\boldsymbol{k}-\boldsymbol{Q}/2|\varepsilon)-E\hat{\mathbf{I}}_{12} \end{bmatrix} \begin{bmatrix} \hat{u}_{k} \\ \hat{u}_{k+Q} \\ u_{k-Q/2} \\ u_{k+Q/2} \end{bmatrix} = 0 \tag{14}$$

where $\hat{\mathbf{I}}_l$ is a $l \times l$ unit matrix, $\hat{u}_k$, $\hat{u}_{k+Q}$, etc are the 1×6 column matrices of the $u_{nk\sigma}$ coefficients.

4. Energy terms at the Γ and L points

In the III–V–VI$_2$ cubic disordered phase as well as in the IV–VI actual energy extrema are located at the L points in the Brillouin zone of the FCC lattice [17]. After ordering of the cations the L points, which are equivalent in the cubic disordered phase, separate into two groups. The first includes two L points located at a chosen spatial cubic diagonal. In the rhombohedral lattice they are brought into coincidence with the Γ point (000) by means of the new reciprocal lattice vector $\boldsymbol{Q}/2$. The remaining L points of the second group are united with the X points of the FCC phase by means of the vector $\boldsymbol{Q}/2$. The equivalence of the points $L=(\pi/2a)$ (111) and $\Gamma=(000)$ as well as $L=(\pi/2a)$ (1−1−1) and $X=(\pi/a)$ (001) is seen visually in figure 2.

Thus, in the III–V–VI$_2$ rhombohedral phase one might expect the band extrema to be located at the L and Γ points of the Brillouin zone.

4.1. Point Γ

Taking into account the Γ point symmetry we may separate the 24th order secular determinant into two 12th order ones of the form (15), where

$$\begin{vmatrix} -E_{-}\hat{\mathbf{I}}_3+(W_{-}+\varepsilon_0)\hat{\mathbf{T}}+\lambda\hat{\mathbf{D}} & 0 & 2(\Sigma_0\hat{\mathbf{I}}_3+W_1\hat{\mathbf{T}}+\lambda^{\Sigma}\hat{\mathbf{D}}) & 2(W_2\hat{\mathbf{T}}+\Sigma_1\hat{\mathbf{I}}_3) \\ 0 & -E_{+}\hat{\mathbf{I}}_3+(W_{+}+\varepsilon_0)\hat{\mathbf{T}}+\lambda_{+}\hat{\mathbf{D}} & 0 & 0 \\ 2(\Sigma_0\hat{\mathbf{I}}_3+W_1\hat{\mathbf{T}}+\lambda^{\Sigma}\hat{\mathbf{D}}) & 0 & (-E_{-}+\eta_{-})\hat{\mathbf{I}}_3+\lambda_{-}\hat{\mathbf{D}}+\varepsilon_0\hat{\mathbf{T}} & \xi\hat{\mathbf{I}}_3+\varepsilon\hat{\mathbf{T}} \\ 2(W_2\hat{\mathbf{T}}+\Sigma_1\hat{\mathbf{I}}_3) & 0 & \xi\hat{\mathbf{I}}_3+\varepsilon\hat{\mathbf{T}} & (-E_{+}+\eta_{+})\hat{\mathbf{I}}_3+\lambda_{+}\hat{\mathbf{D}}+\varepsilon_0\hat{\mathbf{T}} \end{vmatrix} = 0 \tag{15}$$

$$E_{\pm} = E \pm \Delta_0 \qquad W_{\pm} = W \mp W^{\Delta} \qquad \lambda_{\pm} = \lambda \mp \lambda^{\Delta} \qquad \varepsilon = \varepsilon_1 + \varepsilon_2$$

$$\eta_{\pm} = 2(\eta_1 \mp \eta_1^{\Delta}) + (\eta_2 \mp \eta_2^{\Delta}) \qquad \xi = \xi_0 + 2\xi_1$$

$$\Sigma_0 = \tfrac{1}{2}\Sigma^1_{xx}(000) + 2\Sigma^1_{xx}(1-10) + \Sigma^1_{xx}(01-1),$$

$$\Sigma_1 = \Sigma^1_{xx}(100) + 2\Sigma^1_{xx}(010)$$

$$W_1 = \tfrac{1}{2}\Sigma^1_{xy}(000) + \Sigma^1_{xy}(1-10) + 2\Sigma^1_{xy}(10-1)$$

$$W_2 = \Sigma^1_{xy}(100) + \Sigma^1_{xy}(010) + \Sigma^1_{xy}(001)$$

$$\hat{\mathbf{T}} = \begin{bmatrix} -1 & 0 & 0 \\ 0 & -1 & 0 \\ 0 & 0 & 2 \end{bmatrix} \qquad \hat{\mathbf{D}} = \begin{bmatrix} 1 & 0 & 0 \\ 0 & -1 & -\sqrt{2} \\ 0 & -\sqrt{2} & 0 \end{bmatrix}.$$

Here we used the designations: $\Sigma^1_{n'n}(l, q, r) = \langle p_{n'}(\boldsymbol{r})|\Sigma(\boldsymbol{r})|p_n(\boldsymbol{r}-\boldsymbol{R}_{\mathrm{m}})$, $\Sigma^2_{n'n}(l, q, r) = \langle p_{n'}(\boldsymbol{r})|\Sigma(\boldsymbol{r}+\boldsymbol{\tau})|p_n(\boldsymbol{r}-\boldsymbol{R}_{\mathrm{m}})\rangle$ where l, q, r are integers and $R_{\mathrm{m}} = a(lqr)$.

As follows from the form of the matrices $\hat{\mathbf{T}}$ and $\hat{\mathbf{D}}$ the secular determinant (15) is separated into three determinants, two of them are third order and one is sixth order. The roots of the equation $|-E_+\hat{\mathbf{I}}_3 + (W_+ + \varepsilon_0)\hat{\mathbf{T}} + \lambda_+\hat{\mathbf{D}}| = 0$ are easy to find. They define the first set of the Γ-terms

$$\begin{aligned} E^+_{0(\Gamma)} &= -\Delta_0 + \lambda_+ - (W_+ + \varepsilon_0), \\ E^+_{1,2(\Gamma)} &= -\Delta_0 + \tfrac{1}{2}(W_+ + \varepsilon_0 - \lambda_+) \pm \tfrac{1}{2}[9(W_+ + \varepsilon_0)^2 + 6(W_+ + \varepsilon_0)\lambda_+ + 9\lambda_+^2]^{1/2}. \end{aligned} \tag{16}$$

These levels are generated from the valence bands at the L points of the FCC phase. The $\Sigma(\boldsymbol{r})$ potential has no effect on them. This fact is a consequence of its symmetry rather than of the suppositions used.

Three other energy levels are found by solving the cubic equation corresponding to the second third-order determinant.

Among the terms obtained from the sixth-order determinant there is one originated from the E_2^- L term of the FCC phase [3] that together with $E^+_{1(\Gamma)}$ from (16) defined the gap at the Γ point. But the equation of degree 6 cannot be solved analytically. So we have to use perturbation theory. The analysis of the term position at the L- and Γ points of the FCC phase showed [18] that the levels at the L point are situated nearer to the middle of the forbidden gap than the Γ terms. At least the E_2^- level is far enough from the Γ terms. So for the terms forming the conduction band extremum at the Γ point we get

$$\tilde{E}^-_{2(\Gamma)} = E^-_{2(\Gamma)} + \sum_{i=1}^{4} \frac{\tilde{B}^2_{1i}}{E^-_{2(\Gamma)} - E^{\Gamma}_i} \tag{17}$$

where $E^-_{2(\Gamma)}$ is the root of the first diagonal block (15) (the expressions for $E^-_{i(\Gamma)}$ follow from (16) by replacing index '+' by '−' and Δ_0 by $-\Delta_0$), E_i^{Γ} defines the set of Γ levels of the FCC phase, $\tilde{B}_{1i}$ are the transformed non-diagonal block elements (15).

As follows from (16), under deformation $\varepsilon_0 < 0$ the levels $E^+_{1(\Gamma)}$ and $E^-_{2(\Gamma)}$ are shifted downwards in energy, the forbidden gap $E_{g\Gamma}$ being increased in comparison with the E_g of the FCC phase. Under influence of the $\Sigma(\boldsymbol{r})$ potential the $E^-_{2(\Gamma)}$ term (17) is shifted downwards in energy as well. But that shift does not compensate for the increase of $E_{g\Gamma}$

under deformation. As a result the $E_{g\Gamma}$ is increased in comparison with the E_g of the FCC phase. When inverting the terms the $E_{g\Gamma}$ decreases under deformation. Therefore for small $\Sigma(r)$ the energy gap at the Γ point can be smaller than that in the FCC phase. But for large $\Sigma(r)$ the $E_{g\Gamma}$ increases.

4.2. L point

In the FCC phase the symmetry for the L point is D_{3d}, but for the X point it is D_{4h}. After superposition of them in the rhombohedral lattice at the intersection of small D_{3d} and D_{4h} a new small group C_{2h} arises. Its irreducible representations characterise the band states at the L point in the Brillouin zone of the rhombohedral lattice.

The calculation of the L terms has been carried out for point L = $(\pi/2a)$ $(1-1-1)$, which after including the $\Delta(r)$ potential becomes equivalent to L = $(\pi/2a)$ (-111). In its turn the $\Sigma(r)$ brings them into coincidence with the points X = (π/a) (100) and M = (π/a) $(0-1-1)$. The secular determinant for the L point has the form

$$\begin{vmatrix} \hat{H}(\boldsymbol{k}_L|\varepsilon) - E\hat{\mathbf{I}}_{12} & \hat{\Sigma}(\boldsymbol{k}_L) \\ \hat{\Sigma}^+(\boldsymbol{k}_L) & \hat{H}(\boldsymbol{k}_M|\varepsilon) - E\hat{\mathbf{I}}_{12} \end{vmatrix} = 0. \tag{18}$$

Analogous to the Γ point after some unitary transformations the $\hat{H}(\boldsymbol{k}_L|\varepsilon)$ block from (18) becomes quasi-diagonal, the $\Sigma(r)$ potential having no effect on one from its term sets. The energy levels

$$\begin{aligned} E^+_{0(L)} &= 2\sqrt[3]{\rho^+}\cos(\varphi_+/3) - \Delta_0 \\ E^+_{1(L)} &= 2\sqrt[3]{\rho^+}\cos(\varphi_+/3 - 2\pi/3) - \Delta_0 \\ E^+_{2(L)} &= 2\sqrt[3]{\rho^+}\cos(\varphi_+/3 + 2\pi/3) - \Delta_0 \end{aligned} \tag{19}$$

where

$$\cos\varphi_+ = [(W_+ + \varepsilon_0)(W_+ - \varepsilon_0)^2 - \lambda_+^3]/\rho^+$$

$$\rho^+ = (W_+^2 - \tfrac{2}{3}W_+\varepsilon_0 + \varepsilon_0^2 + \lambda_+^2)^{3/2},$$

determine the first term set generated from the valence L bands of the FCC phase.

The $E^+_{1(L)}$ level determines the highest valence band at the L point. In its turn the lowest conduction band is determined by the term

$$\tilde{E}^-_{2(L)} = E^-_{2(L)} + \sum_{j=1}^{3}\left(\frac{|C_{2j}|^2}{E^-_{2(L)} - E'_{xj}} + \frac{|D_{2j}|^2}{E^-_{2(L)} - E''_{xj}}\right), \tag{20}$$

where $E^-_{2(L)}$ has the same form as $E^+_{2(L)}$ (19) with the index '+' replaced by '−' and Δ_0 replaced by $-\Delta_0$; $E'^{(\prime\prime)}_{xj}$ are two sets of the terms at the X point of the deformed FCC phase; C_{2j} and D_{2j} are the matrix elements of the transformed matrix $\boldsymbol{\Sigma}(\boldsymbol{k}_L)$.

It should be noted that for the L point the use of the perturbation theory is more justified than for the Γ point as far as the X levels of the FCC phase are situated much further from the L-terms than the Γ levels.

Analysis of the displacement of the L terms originating the band extrema in com-

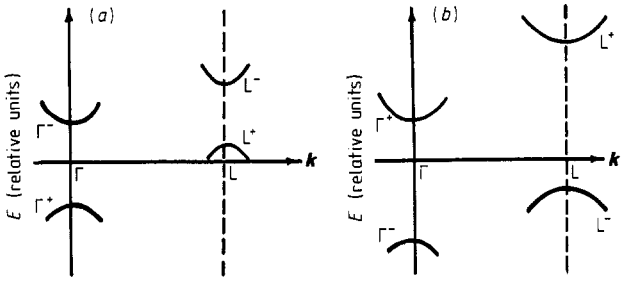

Figure 3. A qualitative picture of the band spectrum of the III–V–VI_2 rhombohedral compounds near the middle of the gap for the (*a*) normal and (*b*) inverted positions of the levels.

Table 2. The interpolation parameters and energy gaps (in units of eV) in the spectrum of $TlB^{V}C_2^{VI}$ compounds (B ≡ Bi, Sb, C ≡ Se, Te).

Parameter	$TlBiSe_2$	$TlBiTe_2$	$TlSbTe_2$
λ_-	0.554	0.554	0.340
λ_+	0.140	0.280	0.280
W_-	−0.315	−0.090	−0.075
W_+	0.650	0.290	0.380
Δ_0	1.380	1.000	0.500
ξ_0	3.170	3.245	3.205
ξ_1	−0.900	−0.900	−0.900
Σ_0	0.200	0.200	0.944
λ^{Σ}	0.182	0.182	−0.061
ε_0	−0.185	−0.088	−0.100
$E_{g\Gamma}$	0.30	0.21	−0.62
E_{gL}	0.06	0.10	−0.66

parison with their position in the FCC phase shows that for the normal term positions ($E_{2L}^{-} > E_{1L}^{+}$) under deformation ($\varepsilon_0 < 0$) and the $\Sigma(r)$ potential the levels E_{1L}^{+} and E_{2L}^{-} converge, but for inverted position they diverge.

As a result of this analysis the qualitative picture of the band spectrum of the III–V–VI_2 rhombohedral compounds near the middle of the gap is shown in figure 3.

5. Model parameters and energy gaps of III–V–VI_2 compounds

In the frame of the p model the electronic energy spectrum is determined by the group of the phenomenological parameters mentioned above. They can be separated into two groups: the FCC phase parameters and those for the rhombohedral phase. For III–V–VI_2 compounds the first group can be well interpolated [17] on the known parameters of the IV–VI semiconductors and Bi-type semimetals [3, 14]. For example, the ionic parameter Δ_0 is determined by the atomic one $\Delta_{at} = \mathcal{I}_c/2 - (\mathcal{I}_A + \mathcal{I}_B)/4$ ($\mathcal{I}_{A,B,C}$ are the ionising potentials of the atomic p terms). The dependence $\Delta_0 = f(\Delta_{at})$ is linear for the IV–VI semiconductors [3], allowing us to find Δ_0 for the III–V–VI_2 ternary disordered phases by means of a value Δ_{at} obtained from the atomic characteristics. The constant λ_+ is equal to the chalcogen spin–orbit splitting, but $\lambda_- = (\lambda_A + \lambda_B)/2$ (λ_A, λ_B are the constants λ for the metal atoms). To determine the parameters $W_\pm$ their linear dependences from lattice constants obtained for IV–VI compounds were used. The values ξ_0 and ξ_1 are the same for all group V materials [3, 14].

As to the second group of parameters, because of the absence of the experimental data we restricted ourselves to the most important ones. The parameter $\Sigma_0 = \Sigma^1_{xx}(000)$ can be found by analogy with Δ_0 from the formula $\Sigma_0 = (\mathcal{I}_A - \mathcal{I}_B)/2$. The displacement potential in $\Sigma(r)$ can be taken into account by means of the parameters for semimetals [14]. The parameter λ^Σ was defined as a half-difference of the spin–orbit splitting constants of the A^{III} and B^V atoms. Finally the parameter ε_0 (deformation parameter) was calculated by the formula $\varepsilon_0 = \varepsilon_{xy} D_0$ (for the deformation potential constant D_0 we used the constants for IV–VI compounds using the principle of isoelectronic analogy).

Using the obtained set of the parameters, the numerical calculations of the energy gaps for the III–V–VI$_2$ compounds were performed. These data as well as the values of the interpolation parameters for three of them are given in table 2.

Several important conclusions follow from table 2. First, the $TlB^VC_2^{VI}$ rhombohedral compounds are narrow-gap semiconductors, their band spectrum being indirect. Secondly, the $E_{g\Gamma}$ and E_{gL} energy gaps being small, the dispersion law should be rather non-parabolic. At last the $TlBiC_2^{VI}$ energy spectrum is normal ($E_{gL} > 0$, $E_{g\Gamma} > 0$), but the

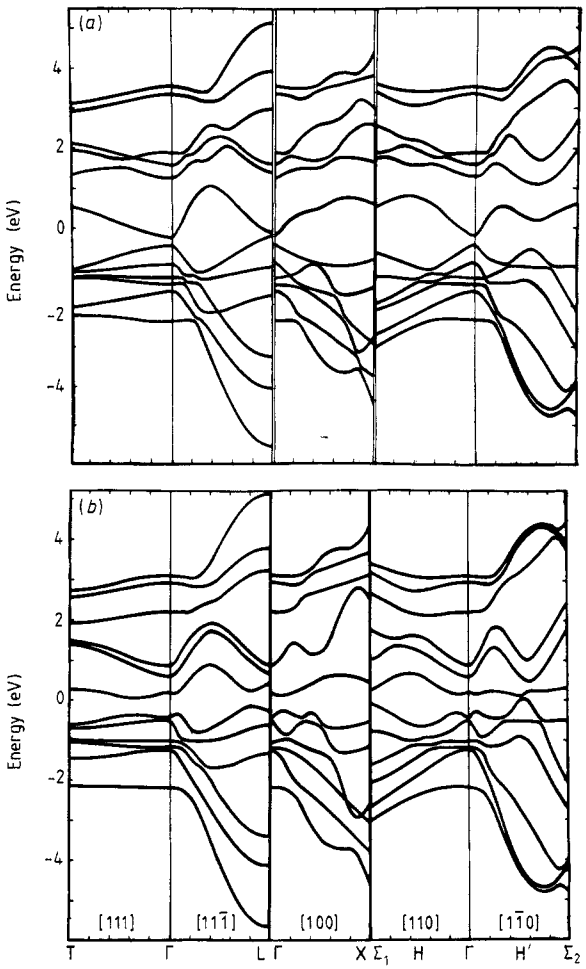

Figure 4. The band structure of (*a*) $TlBiTe_2$ and (*b*) $TlSbTe_2$.

$TlSbC_2^{VI}$ one is inverted ($E_{gL} < 0$, $E_{g\Gamma} < 0$). We should also note that the inverted nature of the $TlSbC_2^{VI}$ spectrum is connected with the small value of the ionicity Δ_0; that is, the band spectrum inversion in the rhombohedral phase is the result of its inversion in the cubic disordered phase.

The bands of the $TlBiTe_2$ and $TlSbTe_2$ compounds along the [111] (T–Γ), [11$\bar{1}$] (Γ–L), [100] (Γ–X), [110] (Γ–Σ_1) and [1$\bar{1}$0] (Γ–Σ_2) directions calculated numerically from (19) are shown in figure 4. These compounds are seen to be the narrow-gap indirect semiconductors with an L valence band and a Γ conduction band. Figure 4 shows one more local extremum group at the H′ point along [1$\bar{1}$0]. In the frame of the p model the H′ extrema are generated from the Σ extrema of $TlB^VC_2^{VI}$ in the cubic phase which are analogous to the Σ extrema of the cubic IV–VI phase. However, the Σ extrema energies are determined by small second-neighbour interactions, so their values calculated from (19) are only rough estimates. It should be noted that in [19] for E_g of the $TlBiTe_2$ compound the value 0.1 eV is given, that, as it is seen from table 2, is in rather good agreement with the obtained theoretical value E_{gL}. However to get the full picture of the band spectrum the model parameter should be defined more exactly by fitting experimental and theoretical data.

Acknowledgments

The authors wish to express their appreciation to B A Volkov and O A Pankratov for helpful discussions.

References

[1] Slater J C and Koster G J 1954 *Phys. Rev.* **94** 1498
[2] Harrison W A 1980 *Electronic Structure and the Properties of Solids* (San Francisco: Freeman)
[3] Pankratov O A and Volkov B A 1987 *Sov. Sci. Rev. Acad. Phys.* **9** 355
[4] Robertson J 1983 *Phys. Rev.* B **28** 4671
[5] Kolomiets B T and Goryunova I A 1955 *Zh. Tekh. Fiz.* **25** 984
[6] Kolomiets B T, Lebedev A A and Taksami I A 1969 *Fiz. Tekh. Poluprov.* **3** 731
[7] Dembovsky S A, Lisovsky L G, Bunin V M and Kanisheva A S 1969 *Izv. Acad. Nauk.* **5** 2023
[8] Hockings F F and White J C 1961 *Acta Crystallogr.* **14** 328
[9] Rey N, Jumas J C, Oliver-Fourcade J and Philippot E 1983 *Acta Crystallogr.* C **39** 971
[10] Popovich N S, Shura V K and Gitsu D V 1983 *J. Cryst. Growth* **61** 406
[11] Feigelson R S and Route R K 1979 *Soc. Photo-Optical Instr. Engg.* **214** 76–9
[12] Paraskevopoulos K M 1985 *J. Phys. C: Solid State Phys.* **18** 4941
[13] Valassiades O, Polychniadis E K, Stoemenos J and Economou N A 1981 *Phys. Status Solidi* a **65** 215
[14] Volkov B A, Falkovsky L A 1983 *Zh. Eksp. Teor. Fiz.* **85** 2135
[15] Jones H 1960 *The Theory of Brillouin Zones and Electronic States in Crystals* (Amsterdam: North Holland)
[16] Bir G L and Pikus G E 1972 *Simmetriya i Deformatsionnye Effecty v Polyprovodnikakh* (transl. *Symmetry and Deformed Effects in Semiconductors*) (Moscow: Nauka)
[17] Kantser V G, Malkova N M and Sidorenko A S 1985 *Solid State Commun.* **56** 513
[18] Gitsu D V, Kantser V G and Malkova N M 1985 *Preprint* (Inst. Prikladnoii Fiz. Acad. Nauk. MSSR) Kishinev
[19] Paraskevopoulos K M 1987 *J. Mater. Sci. Lett.* **6** 1422